Linear and nonlinear electrostatic modes in a strongly coupled quantum plasma

Samiran Ghosh, Nikhil Chakrabarti, and P. K. Shukla

Citation: Phys. Plasmas **19**, 072123 (2012); doi: 10.1063/1.4739782
View online: http://dx.doi.org/10.1063/1.4739782
View Table of Contents: http://pop.aip.org/resource/1/PHPAEN/v19/i7
Published by the American Institute of Physics.

Linear and nonlinear electrostatic modes in a strongly coupled quantum plasma

Samiran Ghosh,[1,a)] Nikhil Chakrabarti,[2,a)] and P. K. Shukla[3,a)]
[1]*Department of Applied Mathematics, University of Calcutta, 92, Acharya Prafulla Chandra Road, Kolkata 700 009, India*
[2]*Saha Institute of Nuclear Physics, 1/AF, Bidhannagar, Kolkata 700 064, India*
[3]*International Center for Advanced Studies in Physical Sciences and Institute for Theoretical Physics, Faculty of Physics & Astronomy, Ruhr University Bochum, D-44780 Bochum, Germany and Department of Mechanical and Aerospace Engineering & Centre for Energy Research, University of California San Diego, La Jolla, California 92093, USA*

(Received 31 May 2012; accepted 11 July 2012; published online 30 July 2012)

The properties of linear and nonlinear electrostatic waves in a strongly coupled electron-ion quantum plasma are investigated. In this study, the inertialess electrons are degenerate, while non-degenerate inertial ions are strongly correlated. The ion dynamics is governed by the continuity and the generalized viscoelastic momentum equations. The quantum forces associated with the quantum statistical pressure and the quantum recoil effect act on the degenerate electron fluid, whereas strong ion correlation effects are embedded in generalized viscoelastic momentum equation through the viscoelastic relaxation of ion correlations and ion fluid shear viscosities. Hence, the spectra of linear electrostatic modes are significantly affected by the strong ion coupling effect. In the weakly nonlinear limit, due to ion-ion correlations, the quantum plasma supports a dispersive shock wave, the dynamics of which is governed by the Korteweg-de Vries Burgers' equation. For a particular value of the quantum recoil effect, only monotonic shock structure is observed. Possible applications of our investigation are briefly mentioned. © *2012 American Institute of Physics*. [http://dx.doi.org/10.1063/1.4739782]

I. INTRODUCTION

The physics of quantum plasmas[1,2] is of considerable interest because of its novelty, and its potential applications in modern technology (e.g., in intense laser compressed plasma experiments, in pulsed thermonuclear fusion, in semiconductor and metallic nanostructure plasmas, etc.), in planetary systems (e.g., the core of the planet Jupiter) and in dense astrophysical objects (e.g., giant stars, neutron stars, quark stars, magnetars, white dwarfs, etc.[2–9] A dense plasma can be described as a quantum fluid when its macroscopic properties, viz., the plasma number density, are significantly high so that the electrons are degenerate. In the crust of neutron stars and in the cores of white dwarfs, different types of ionic crystals (fully ionized carbon, oxygen, iron, etc.) embedded into degenerate Fermi gas of electrons (the quantum statistical electron force is significant as the Fermi electron temperature T_{F_e} is much higher than the plasma electron temperature T_e) are observed.[10] Thus, such dense astrophysical plasmas can be regarded as strongly correlated quantum plasmas.[11] Recently, experimental observations[12] of the low-temperature ultra-cold two-component (electron-ion) plasmas and the achievement of $T_e/T_{F_e} \sim 1$ in experiments[13] indicate the possibility of observation of strongly coupled quantum plasmas (SCQPs) in the laboratory.[14] Here, strong coupling is defined in terms of the usual Coulomb coupling parameter $\Gamma_s = e^2/\epsilon_0 a_s T_s$, where e is the magnitude of the electron charge, T_s the temperature (in energy units) of the plasma species s, $a_s = (3/4\pi n_s)^{1/3}$ the inter-particle distance (the Wigner-Seitz radius) of the species s, and n_s the number density of the species s. The plasma is regarded as weakly coupled if $\Gamma_s \ll 1$, and strongly coupled if $\Gamma_s \gg 1$.

In a weakly coupled quantum plasma, the low-frequency electrostatic (LF-ES) modes (e.g., the ion acoustic wave (IAW)[15] and the electron acoustic wave[16]) have been investigated within the framework of the quantum hydrodynamical model (QHM).[17–19] The low-frequency dust acoustic waves in a classical strongly correlated plasma with non-degenerate electrons, ions, and charged dust grains have also been observed in dusty plasmas.[20–25] The necessary condition for the existence of a plasma crystal in a strongly correlated one component plasma (OCP) with quantum effects and its collective behavior have also been investigated.[2,26–30] The fundamental properties of one component SCQPs and two-component SCQPs differ qualitatively.[11] Therefore, it is pertinent to investigate the characteristics of collective modes in two-component SCQPs.

In this paper, we investigate the propagation characteristics of the LF-ES modes in electron-ion SCQPs. The ions are non-degenerate and strongly correlated. The ion dynamics is governed by a phenomenological generalized hydrodynamical (GH) model. The electrons are degenerate and weakly correlated. The electron dynamics is described by the QHM. By using the continuity equations together with the GH and QH models and Poisson's equation, we derive the general dispersion relation for the LF-ES modes in SCQPs. The

[a)]Electronic addresses: sran_g@yahoo.com, nikhil.chakrabarti@saha.ac.in, and profshukla@yahoo.de.

dispersion relation is analyzed both theoretically and numerically. Furthermore, we investigate the nonlinear propagation characteristics of one spatial dimension (1D) LF-ES waves in our quantum plasma. In the weakly nonlinear limit, ion-ion correlation effects introduce a viscous dissipation that is responsible for the emergence of a Korteweg-de Vries Burgers (KdVB) equation that governs the dynamics of the finite amplitude LF-ES modes. The quantum recoil effect provides corrections to the usual dispersive character of the waves. Analytical and numerical solutions reveal the existence of dispersive (oscillatory) shock wave in SCQPs. However, for a particular value of the quantum recoil parameter, the system supports only a monotonic shock like structure.

The manuscript is organized in the following fashion. Physical assumptions and the basic equations to describe the model are discussed in Sec. II. The linear properties of the LF-ES modes are discussed in Sec. III. The weakly nonlinear LF-ES wave propagation characteristics are discussed in Sec. IV. Finally, a brief summary of our results and their possible applications are presented in Sec. V.

II. PHYSICAL ASSUMPTIONS AND GOVERNING EQUATIONS

The plasma is quasi-neutral, i.e., $Zn_{i0} = n_{e0}$, where $n_{e(i)0}$ is the equilibrium number density of electrons (ions) and Z the ion charge state. The physical assumptions to formulate our problem are as follows:

(1) The degeneracy (dimensionless) parameter for a particle species s is defined as

$$\chi_s \equiv \frac{\varepsilon_{F_s}}{T_s} = \frac{1}{2}(3\pi^2)^{2/3}(n_{so}\lambda_{B_s}^3)^{2/3},$$

where $\varepsilon_{F_s}(= \hbar^2(3\pi^2 n_{s0})^{2/3}/2m_s$, m_s is the mass of the particle species s, and $\lambda_{B_s}(= \hbar/\sqrt{m_s T_s})$ are the Fermi energy in the ground state and thermal de Broglie wavelength of the particle species s, respectively.

(a) The electrons are fully degenerate, i.e., the electron Fermi energy (ε_{F_e}) is much larger than the electron thermal energy (T_e), so that the electron degeneracy parameter $\chi_e \gg 1$. This implies that

$$n_{i0} \gg \frac{1}{3\pi^2}\left(\frac{2m_e T_e}{\hbar^2}\right)^{3/2} = n_Q.$$

Note that we here also assume that the electrons are non-relativistic, i.e., $\varepsilon_{F_e} \ll m_e c^2$, where c is the speed of light in vacuum.

(b) The ions are non-degenerate, i.e., the Fermi ion energy (ε_{F_i}) is much smaller than the ion thermal energy (T_i), so that the ion degeneracy parameter $\chi_i \ll 1$. This implies that

$$n_{i0} \ll \frac{1}{3\pi^2}\left(\frac{2m_i T_i}{\hbar^2}\right)^{3/2} = \bar{n}_Q.$$

(2) The ions are strongly correlated, so that the ion coupling parameter

$$\Gamma_i = \left(\frac{1}{n_{i0}\lambda_{D_i}^3}\right)^{2/3} = \frac{Z^2 e^2}{\epsilon_0 a_i T_i} \gg 1,$$

where $\lambda_{D_i}(= \sqrt{\epsilon_0 T_i/n_{i0}Z^2e^2})$ is the ion Debye radius and $a_i(= (3/4\pi n_{i0})^{1/3})$ is the inter-ionic distance. This implies that

$$n_{i0} \gg \frac{3}{4\pi}\left(\frac{Z^2e^2}{\epsilon_0 T_i}\right)^{-3} = n_{SC}.$$

(3) The electron correlations are neglected as the electron-electron correlation effects are negligibly small compared to ion-ion correlations. This can be easily seen from the relation

$$\Gamma_e = \left(\frac{1}{n_{e0}\lambda_{F_e}^3}\right)^{2/3} = 1.5Z^{-5/3}\chi_e^{-1}\theta\Gamma_i \ll \Gamma_i$$

as $\chi_e \gg 1$, $Z \geq 1$, and $\theta(= T_i/T_e) \leq 1$. Here, $\lambda_{F_e}(= v_{F_e}/\sqrt{3}\omega_{pe})$ is the Thomas-Fermi three-dimensional (3D) screening length of electrons, $v_{F_e}(= \sqrt{2\varepsilon_{F_e}/m_e})$ the Fermi speed of electrons, and $\omega_{pe}(= \sqrt{n_{e0}e^2/\epsilon_0 m_e})$ the electron plasma frequency. The electron-ion interactions are weak compared to ion-ion correlations, when the ion dynamics is considered, and, therefore, we can neglect the electron-ion interactions.

The assumptions (1) and (2) determine a highly dense $[\max\{n_Q, n_{SC}\} \ll n_{i0} \ll \bar{n}_Q]$ quantum plasma system. If the plasma temperature exceeds 1 eV, (say) for a typical hydrogen plasma with $\theta = 1$, the assumptions are valid as long as the plasma number density $n_{i0} \sim (10^{28} - 10^{32})\mathrm{m}^{-3}$. Thus, the physical system considered here is highly dense ($\Gamma_i \gg 1$; strongly coupled) plasma in which the electrons form a degenerate quantum fluid with weak interactions, while the ions form a classical fluid with strong interactions.

To model the strongly correlated ion dynamics, we use the viscoelastic approach which is described by the non-Markovian GH model.[2,21,25,31] Accordingly, we consider the following generalized momentum equation for the ion fluid, viz.,

$$\left(1 + \tau_m \frac{d}{dt}\right)\left[m_i n_i \frac{dv}{dt} + \nabla p_i - Zen_i\mathbf{E}\right] = \eta\nabla\cdot\nabla v + \left(\varsigma + \frac{\eta}{3}\right)\nabla(\nabla\cdot v), \quad (1)$$

where $d/dt \equiv \partial/\partial t + v\cdot\nabla$, $\mathbf{v}$ is the ion fluid velocity, $\mathbf{E}$ the electric field, n_i the unperturbed ion number density, p_i the ion pressure, η the shear viscosity coefficient, ς the bulk viscosity coefficient, and τ_m the viscoelastic relaxation time or a memory function.

In addition to the above generalized momentum equation (1), the GH model includes the ion continuity equation

$$\frac{\partial n_i}{\partial t} + \nabla\cdot(n_i v) = 0 \quad (2)$$

and the energy equation. However, the ion dynamics is isothermal at strong couplings,[26] and therefore the ion energy

equation is redundant. The ion pressure gradient becomes $\nabla p_i = T_i \mu_i \nabla n_i$, where $\mu_i [= (1/T_i)(\partial p_i/\partial n_i)_{T_i}] = 1 + u(\Gamma_i)/3 + (\Gamma_i/9)\partial u(\Gamma_i)/\partial \Gamma_i$ is the isothermal compressibility factor for ion fluid. The function $u(\Gamma_i)$ is the measure of the excess internal energy of the system, which is related to the correlation energy E_c by $u = E_c/n_{i0}T_i$. In the framework of the OCP model, $u(\Gamma_i) \approx -0.9\Gamma_i$ (for $\Gamma_i \gg 1$).[27] In the pressure term, this non-thermal contribution prevails over the temperature that leads to thermodynamic instability (artifact instability).[21,30] However, this difficulty does not arise in our two-component plasma model. For the two-component plasma, the cellular model yields $u(\Gamma_i) = \Gamma_i(-0.9 + 1.5(r_i/a_i)^2)$,[32] where r_i is the ion core radius, which depends on the degree of ion striping.

The electron fluid is fully degenerate (strongly quantum) and weakly coupled (compared to the ion coupling). Therefore, we consider QHM for the electron dynamics. Moreover, for the LF-ES modes ($\omega \ll \omega_{pe}$), we neglect the electron inertia in the QHM for the electrons and have the momentum conservation equation for the electrons as

$$0 = -e\mathbf{E} - \frac{\nabla p_e}{n_e} + \frac{\hbar^2}{2m_e}\nabla\left(\frac{\nabla^2\sqrt{n_e}}{\sqrt{n_e}}\right). \tag{3}$$

In the above, the term containing $\hbar^2$ arises due to the quantum recoil effect (viz., electron tunneling through the Bohm potential), n_e is the unperturbed electron number density, and p_e the electron pressure. Here, following,[33] we assume that the electrons obey the equation of state pertaining to 3D zero temperature Fermi gas, which is given by $p_e = m_e v_{F_e}^2 n_e^{5/3}/5n_{e0}^{2/3}$.

The system of equations is closed by Poisson's equation

$$\nabla \cdot \mathbf{E} = \frac{e}{\epsilon_0}(Zn_i - n_e). \tag{4}$$

III. LINEAR MODES

Here, we derive a general dispersion relation for the LF-ES modes in our two component SCQPs. Then, the dispersion relation is analyzed both analytically and numerically.

A. The dispersion relation

For the linear LF-ES modes, we perturb the system with a small amplitude disturbance, i.e., we let $v = 0 + v_1$, $\mathbf{E} = 0 + \mathbf{E}_1$, $n_{e(i)} = n_{e(i)0} + n_{e(i)1}$, where all the variables with subscript 1 are perturbations. Linearizing equations (1)–(4), and using Fourier transform of all the perturbed variables [$\sim \exp(i\mathbf{k}\cdot\mathbf{r} - \omega t)$, ω is the frequency and $\mathbf{k}$ is the wave vector of the mode under consideration], we derive the electron ($\alpha_e(k,\omega)$) and ion ($\alpha_i(k,\omega)$) susceptibilities. Introducing the dimensionless quantities, $k(=|\mathbf{k}|) = ka_i$, $\lambda_{F_e} = \lambda_{F_e}/a_i$, $H = 3\hbar\omega_{pe}/2T_{F_e}$ (T_{F_e} in energy unit; $T_{F_e} \equiv \varepsilon_{F_e}$), $\tau_m = \tau_m\omega_{pi}$, $\lambda_{D_i} = \lambda_{D_i}/a_i$, $\omega = \omega/\omega_{pi}$, and $\eta^* = \left(\frac{4}{3}\eta + \varsigma\right)/m_i n_{i0}\omega_{pi}a_i^2$, where $\omega_{pi}(= \sqrt{n_{i0}Z^2e^2/\epsilon_0 m_i})$ is the ion plasma frequency, we express the $\alpha_e(k,\omega)$, $\alpha_i(k,\omega)$ as

$$\alpha_e(k,\omega) = \frac{1}{k^2\lambda_{F_e}^2(1 + H^2k^2\lambda_{F_e}^2/4)} \quad \text{and}$$
$$\alpha_i(k,\omega) = -\frac{1}{\omega^2 - \mu_i k^2\lambda_{D_i}^2 + i\omega\eta_i(k,\omega)}, \tag{5}$$

where H is the dimensionless quantum parameter related to the electron Wigner-Seitz radius in units of the Bohr radius a_B. In the above, $\eta_i(k,\omega)$ is

$$\eta_i(k,\omega) = \frac{\eta^* k^2}{(1 - i\omega\tau_m(k))}. \tag{6}$$

In the (k,ω) space, the memory function $\tau_m(k)$ was given in Ref. 28 and reads

$$\tau_m(k) = \tau_m(0)Y(k), \quad \tau_m(0) = \frac{\eta^*}{\lambda_{D_i}^2}\left[1 - \mu_i + \frac{4}{15}u(\Gamma_i)\right]^{-1}, \tag{7}$$

where $Y(k)(= Y_G(k)) = \exp[-(k/\xi_G)^2]$ for a Gaussian distribution and $Y(k)(= Y_L(k)) = [1 + (k/\xi_L)^2]^{-1}$ for a Lorentzian distribution. Here, ξ_G and ξ_L are the scale factors.[28] Note that, for fixed value of Γ_i, $\tau_m(k)$ decreases rapidly with the wave number k for $Y_G(k)$. Therefore, for computation, it is convenient to use $Y_L(k)$.[28] Hereafter, we shall use $\tau_m(k) \equiv \tau_m$.

The low-frequency dispersion relation for SCQPs can be written as $1 + \alpha_e(k,\omega) + \alpha_i(k,\omega) = 0$, which implies

$$\omega^2 - \mu_i k^2\lambda_{D_i}^2 + \frac{i\omega k^2\eta^*}{(1 - i\omega\tau_m)} = \mathcal{A}, \tag{8}$$

where

$$\mathcal{A} = \frac{k^2\lambda_{F_e}^2(1 + H^2k^2\lambda_{F_e}^2/4)}{1 + k^2\lambda_{F_e}^2(1 + H^2k^2\lambda_{F_e}^2/4)}.$$

In the absence of ion-ion correlation effects ($\eta^* \to 0$) and ion thermal contribution ($\lambda_{D_i} \to 0$), from Eq. (8), we obtain the dispersion relation

$$\omega^2 = \mathcal{A} = \frac{k^2\lambda_{F_e}^2(1 + H^2k^2\lambda_{F_e}^2/4)}{1 + k^2\lambda_{F_e}^2(1 + H^2k^2\lambda_{F_e}^2/4)}, \tag{9}$$

which reveals the dispersion properties of the IAW modified by the quantum diffraction due to electron-tunneling effects. In the literature, this mode is known as the quantum ion acoustic wave (QIAW).[15] In the long wave length limit, viz., $k\lambda_{F_e} \ll 1$, and $H \ll 1$, Eq. (9) yields the well known Bohm-Staver speed,[34]

$$c_{BS} = \frac{v_{F_e}}{\sqrt{3}}\left(\frac{\omega_{pi}}{\omega_{pe}}\right)$$

(in the dimensional form). In absence of ion-ion correlations, viz., ($\eta^* \to 0$), the dispersion relation (8) reduces to

$$\omega^2 = k^2\lambda_{F_e}^2\left[\frac{1 + H^2k^2\lambda_{F_e}^2/4}{1 + k^2\lambda_{F_e}^2(1 + H^2k^2\lambda_{F_e}^2/4)} + \mu_i\left(\frac{\lambda_{D_i}}{\lambda_{F_e}}\right)^2\right],$$

which includes the ion isothermal compressibility correction to the QIAW. Furthermore, in the limits $k\lambda_{F_e} \ll 1$ and $H \ll 1$, we have

$$\omega = kc_{BS}\left(1 + \frac{3\theta\mu_i}{2Z\varepsilon_{F_e}}\right),$$

which is the ion isothermal compressibility correction of the Bohm-Staver formula in our two component quantum plasma. Finally, in the classical limit ($\lambda_{F_e} \to \lambda_{D_e}$ (the electron Debye radius), and $H=0$), $\mathcal{A} \to k^2\lambda_{D_e}^2/(1+k^2\lambda_{D_e}^2)$ and Eq. (9) describes the usual IAW mode

$$\omega = \frac{k\lambda_{D_e}}{\sqrt{1+k^2\lambda_{D_e}^2}}$$

(recall that ω is normalized by ω_{pi}).

Thus, Eq. (8) represents the general dispersion relation for the LF-ES modes in SCQPs in the presence of the quantum diffraction due to electron tunneling. The interesting feature of the non-Markovian GH model is that the dissipative term (the ion fluid viscosity) can be represented by the memory function τ_m (defined in Eq. (7)), which is nonlocal in space and time. In the (k,ω) space, this function tends to the ordinary dissipative term in the low-frequency limit, which is known as the *hydrodynamic regime*. However, at the relatively high-frequency limit τ_m represents some kinetic effects, which is known as the *kinetic regime* in the (k,ω) space. Actually, τ_m provides a characteristic time scale to distinguish two classes of the LF-ES modes: the *hydrodynamic mode* when $\omega\tau_m \ll 1$ and the *kinetic mode* when $\omega\tau_m \gg 1$.

In the *hydrodynamic regime* ($\omega\tau_m \ll 1$), the dispersion relation (8) simplifies to

$$\omega^2 = \mathcal{A} + \mu_i k^2\lambda_{D_i}^2 + i\omega k^2\eta^*, \tag{10}$$

which is solved for the complex frequency $\omega(=\omega_r + i\omega_i)$ and real k. The real and imaginary parts of the frequencies are, respectively,

$$\omega_r = \pm\sqrt{\mathcal{A} + \mu_i k^2\lambda_{D_i}^2 - \omega_i^2}; \quad \omega_i = -\frac{k^2\eta^*}{2}. \tag{11}$$

It follows that that this low-frequency mode suffers viscous damping in the *hydrodynamic regime*, as also observed in strongly coupled dusty plasmas[21,23] with strongly correlated charged dust grains and Boltzmann distributed electrons and ions. The *kinetic regime* ($\omega\tau_m \gg 1$) is relatively high frequency regime bounded by $\tau_m^{-1} \ll \omega \ll \omega_{pe}$. In this regime, the dispersion relation (8) simplifies to

$$\omega^2 = \mathcal{A} + \mu_i k^2\lambda_{D_i}^2 + \left(\frac{\eta^*}{\tau_m}\right)k^2. \tag{12}$$

Note the contrast of the dispersion relation (12) with that of (10) in the *hydrodynamic regime*. Here (in *kinetic regime*) the viscosity is acting as the source of the wave, while in the hydrodynamic regime it simply acts as the dissipating agent.

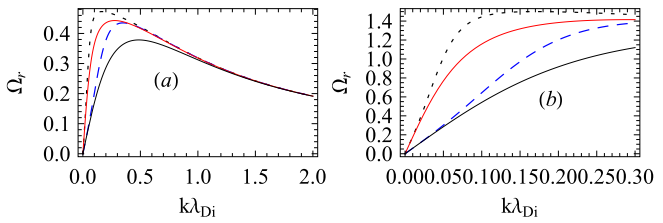

FIG. 1. Normalized real frequency ($\Omega_r = \omega_r\tau_m$) versus $k\lambda_{D_i}$ of the dispersion relation (8) for $H=0$ (solid lines) and $H=4$ (dashed and dotted lines). Solid red and dotted lines for $\theta = 0.1$, whereas solid black and dashed lines for $\theta = 1$. (a) and (b) are drawn for $\Gamma_i = 8$ and $\Gamma_i = 0.8$, respectively.

This is clearly demonstrated from the dispersion relation (12) in the classical limit and cold ion approximation. In the dimensional form, we have from (12)

$$\omega^2 = \frac{k^2c_s^2}{1+k^2\lambda_{D_e}^2} + \frac{k^2\left(\frac{4}{3}\eta + \varsigma\right)}{\tau_m m_i n_{i0}},$$

where c_s is the usual ion sound velocity. Inclusion of a finite ion temperature introduces compressibility effect. Interestingly, the quantum diffraction effect brings the dispersive character in this novel mode which is given as

$$\omega = \pm\left[\mathcal{A} + k^2\lambda_{D_i}^2\left(1 + \frac{4}{15}u(\Gamma_i)\right)\right]^{1/2}, \tag{13}$$

where we have substituted the expressions for η^* and τ_m in Eq. (12). This shows that the *kinetic mode* does not suffer any viscous damping.

B. Numerical solution

Here, we present a more complete picture by exactly solving the dispersion relation (8) for the complex frequency $(\omega = \omega_r + i\omega_i)$ and the real wave number k. Substituting this in Eq. (8), we obtain the following coupled equations for $\omega\tau_m$:

$$y^3 - y^2 + \kappa y - \beta = 0, \quad \text{and} \quad \Omega_r^2 = \frac{\beta}{y} - \left(\frac{y-1}{2}\right)^2, \tag{14}$$

where $\Omega_r = \omega_r\tau_m$, $\Omega_i = \omega_i\tau_m$, $y = 1 + 2\Omega_i$, $\kappa = \beta + \eta^*\tau_m k^2$, and $\beta = \tau_m^2(\mathcal{A} + \mu_i k^2\lambda_{D_i}^2)$. The properties of the LF-ES modes in SCQPs can be made clearer by the computation of Eq. (14) simultaneously. The above simultaneous Eq. (14) is solved for $\Omega_i < 0$. The results are displayed in Figs. 1 and 2 for a range of the coupling parameter Γ_i, the quantum diffraction parameter H, and temperature ratio θ. The frequency

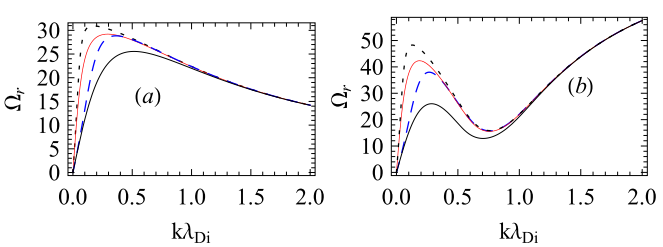

FIG. 2. Same as in Fig. 1. But curves (a) and (b) are drawn for $\Gamma_i = 0.1$ and $\Gamma_i = 180$.

$\Omega_r(=\omega_r\tau_m)$ versus $k\lambda_{D_i}$ is plotted in these figures. In these figures, red solid lines are drawn for $H=0,\theta=0.1$, black solid lines are drawn for $H=0,\theta=1$, dotted lines are drawn for $H=4,\theta=0.1$, and dashed lines are drawn for $H=4,\theta=1$.

The dispersion curves in these figures show that the ion correlation effects, quantum diffraction, and also the electron-ion temperature ratio provide the dispersive corrections through to change the phase velocity of the low-frequency longitudinal modes. The turnover effects of the dispersion curves $(\omega=\omega(k))$ with $\partial\omega/\partial k<0$ also occur in the long wavelength limit. As a consequence, the group velocity of the low frequency modes changes its sign.

The dispersion curves in Fig. 1(a) represent the low frequency *hydrodynamic modes* as $\Omega_r \ll 1(\omega_r\tau_m \ll 1)$. This figure reveals that the SCQP supports *hydrodynamic modes* for $1<\Gamma_i<10$. This is happened due to the fact that η^* decreases as function of Γ_i and displays a broad minimum (~ 1) in this range Γ_i $(1<\Gamma_i<10)$ after that it begins to increase as $\propto \Gamma_i^{4/3}$.[28,32] Curves in Fig. 1(b) show the smooth evolution from the *hydrodynamic regime* $(\Omega_r<1)$ to the *kinetic regime* $(\Omega_r>1)$ with the increase of wave number k. These smooth evolutions from one regime to the other are shown for moderate coupling $\Gamma_i=0.8$.

Figures 2(a) and 2(b) are drawn for $\Gamma_i=0.1$ (weak coupling) and 180 (strong coupling), respectively. This figure shows that the kinetic condition $\Omega_r \gg 1(\omega\tau_m \gg 1)$ is easily satisfied both in weak and in very strong coupling limits. This is because $\tau_m(\propto \eta^*)$ closely follows the behavior of η^*, which is high in the weak coupling as well as in the strong coupling limits.[28,32] Molecular dynamic simulations and liquid-metal experimental data-fitting results indicate that in the weak coupling $\tau_m \propto \Gamma_i^{-3/2}$ (Ref. 26) and in the strong coupling it is $\propto \Gamma_i^{4/3}$.[32]

Thus, the curves in Fig. 2 represent the LF *kinetic modes* in SCQP. The dispersion curves of *kinetic modes* show multiple transition behavior for the high value of Γ_i. The first transition $(\partial\omega/\partial k<0)$ occurs in the long wavelength limit and the other transition $(\partial\omega/\partial k>0)$ occurs in the short wavelength limit. This type transition occurs in the short wavelength range for strong coupling, which indicates the growth of incipient Brillouin zones as the system nears crystallization.[23] Fig. 2 also shows that in acoustic limit ($k \ll 1$, i.e., $k\to 0$), one gets back to the *hydrodynamic regime*. These are clearly shown in Fig. 1(b) for moderate coupling. Therefore, there exists some minimum value of the wave number $(k_{min}\neq 0)$ above which *kinetic modes* are expected to exist. The curves in Fig. 2 (particularly in Fig. 1(b)) exhibit that k_{min} has a functional dependence on Γ_i, H, and θ. This k_{min} decreases with the increase of the coupling parameter (Γ_i) and quantum diffraction (H) due to electron tunneling, whereas it increases with the increase of the electron-ion temperature ratio (θ).

IV. WEAKLY NONLINEAR MODES

We have already seen that the linear LF-ES modes suffer viscous damping due to ion-ion correlations in the *hydrodynamic regime* $(\omega\tau_m \ll 1)$. Thus, it is interesting to see how the ion viscous dissipation affects the weakly nonlinear structures in SCQPs. Here, we investigate the weakly nonlinear localized structures in 1D (generalization to more spatial dimension is straightforward) namely the x-direction in the *hydrodynamic regime*.

A. The nonlinear evolution equation

To investigate the nonlinear structures, it is always convenient to write the governing equations in the dimensionless form; for this, we introduce the following dimensionless variables: $\bar{x}=x/\lambda_{D_i}$, $\bar{t}=\omega_{pi}t$, $n_{e(i)}^{-}=n_{e(i)}/n_{e(i)0}$, and $\bar{v}=v/v_{T_i}$, where $v_{T_i}(=\sqrt{T_i/m_i})$ is the ion thermal speed. Hereafter, we will be using these new variables and remove all the bars for simplicity of notations. Note that in case of 1D, the electrons obey the equation of state pertaining to 1D zero temperature Fermi gas given by $p_e=m_e v_{F_e}^2 n_{e0}(n_e/n_{e0})^3/3$. Finally, in the *hydrodynamic regime* $(\omega\tau_m \ll 1)$, from Eqs. (1) and (3), we obtain

$$\frac{\partial v}{\partial t}+v\frac{\partial v}{\partial x}+\mu_i\frac{\partial \ln n_i}{\partial x}-E=\frac{\eta^*}{n_i}\frac{\partial^2 v}{\partial x^2}, \tag{15}$$

$$\frac{\partial n_i}{\partial t}+\frac{\partial}{\partial x}(n_i v)=0, \tag{16}$$

$$0=-E-\left(\frac{\tilde{\lambda}_{F_e}}{\lambda_{D_i}}\right)^2 n_e\frac{\partial n_e}{\partial x}+\frac{\tilde{H}^2}{2}\left(\frac{\tilde{\lambda}_{F_e}}{\lambda_{D_i}}\right)^4\frac{\partial}{\partial x}\left[\frac{1}{\sqrt{n_e}}\frac{\partial^2\sqrt{n_e}}{\partial x^2}\right], \tag{17}$$

and

$$\frac{\partial E}{\partial x}=n_i-n_e. \tag{18}$$

In the above, $\tilde{H}(H/3=\hbar\omega_{pe}/2T_{F_e})$ is the quantum diffraction due to 1D electron tunneling effect and $\tilde{\lambda}_{F_e}(\sqrt{3}\lambda_{F_e}=v_{F_e}/\omega_{pe})$ is the Thomas-Fermi 1D screening length of electrons. For weak perturbations, the reductive perturbation technique is employed and the following stretched coordinate is introduced

$$\xi=\sqrt{\epsilon}(x-Ut), \quad \tau=\epsilon^{3/2}t, \tag{19}$$

where ϵ is a small nonzero parameter proportional to the amplitude of the perturbation and U the phase speed of the mode normalized by the ion thermal speed. The dynamical variables $n_{e(i)}$, v, and E are expanded about their equilibrium value in power series of ϵ in the following way:

$$\begin{pmatrix} n_{e(i)} \\ v \\ E \end{pmatrix}=\begin{pmatrix} 1 \\ 0 \\ 0 \end{pmatrix}+\epsilon\begin{pmatrix} n_{e(i)}^{(1)} \\ v^{(1)} \\ \sqrt{\epsilon}E^{(1)} \end{pmatrix}+\epsilon^2\begin{pmatrix} n_{e(i)}^{(2)} \\ v^{(2)} \\ \sqrt{\epsilon}E^{(2)} \end{pmatrix}+\cdots. \tag{20}$$

Now, to introduce the effects of ion correlations and to make the nonlinear perturbation consistent with that of (19) and (20), we assume that $\eta^*\sim O(\sqrt{\epsilon})$. Finally, substitution of (19) and (20) into the dynamical equations (15)–(18) leads to the following relations in lowest powers of ϵ:

$$E^{(1)} = \frac{\partial\left(\mu_i n_i^{(1)} - U v^{(1)}\right)}{\partial \xi}, \quad v^{(1)} = U n_i^{(1)}, \qquad E^{(1)} = -\left(\frac{\tilde{\lambda}_{F_e}}{\lambda_{D_i}}\right)^2 \frac{\partial n_e^{(1)}}{\partial \xi}, \quad n_e^{(1)} = n_i^{(1)}. \tag{21}$$

From these relations, we obtain

$$U = \sqrt{\mu_i + \left(\frac{\tilde{\lambda}_{F_e}}{\lambda_{D_i}}\right)^2}. \tag{22}$$

Next, the dynamical equations in the next higher powers of ϵ are obtained as

$$E^{(2)} = \frac{\partial v^{(1)}}{\partial \tau} + v^{(1)} \frac{\partial v^{(1)}}{\partial \xi} - \mu_i n_i^{(1)} \frac{\partial n_i^{(1)}}{\partial \xi} - \eta^* \frac{\partial^2 v^{(1)}}{\partial \xi^2} + \mu_i \frac{\partial n_i^{(2)}}{\partial \xi} - U \frac{\partial v^{(2)}}{\partial \xi}, \tag{23}$$

$$\frac{\partial n_i^{(1)}}{\partial \tau} + \frac{\partial\left(n_i^{(1)} v^{(1)}\right)}{\partial \xi} = U \frac{\partial n_i^{(2)}}{\partial \xi} - \frac{\partial v^{(2)}}{\partial \xi}, \tag{24}$$

$$E^{(2)} = -\left(\frac{\tilde{\lambda}_{F_e}}{\lambda_{D_i}}\right)^2 n_e^{(1)} \frac{\partial n_e^{(1)}}{\partial \xi} - \left(\frac{\tilde{\lambda}_{F_e}}{\lambda_{D_i}}\right)^2 \frac{\partial n_e^{(2)}}{\partial \xi} + \frac{\tilde{H}^2}{4}\left(\frac{\tilde{\lambda}_{F_e}}{\lambda_{D_i}}\right)^4 \frac{\partial^3 n_e^{(1)}}{\partial \xi^3}, \tag{25}$$

and

$$\frac{\partial E^{(1)}}{\partial \xi} = n_i^{(2)} - n_e^{(2)}. \tag{26}$$

Finally, elimination of $n_{e(i)}^{(2)}$, $v^{(2)}$, and $E^{(2)}$ from Eqs. (23)–(26) and using Eq. (21), the following KdVB equation, with $\psi \equiv U n_i^{(1)} / \left(\mu_i + 2(\tilde{\lambda}_{F_e}/\lambda_{D_i})^2\right)$, is obtained

$$\frac{\partial \psi}{\partial \tau} + \psi \frac{\partial \psi}{\partial \xi} + \beta \frac{\partial^3 \psi}{\partial \xi^3} = \mu \frac{\partial^2 \psi}{\partial \xi^2}, \tag{27}$$

where coefficients β and μ can be written in the following simplified form:

$$\beta = \frac{1}{2U}\left(\frac{\tilde{\lambda}_{F_e}}{\lambda_{D_i}}\right)^2 \left(1 - \frac{\tilde{H}^2}{4}\right), \quad \mu = \frac{\eta^*}{2}.$$

Thus, in the SCQPs, the dynamics of the weakly nonlinear LF-ES wave is governed by the KdVB equation (27). The ion-ion correlation effects introduce the Burgers term $\mu(\propto \eta^*)$. The quantum diffraction effect due to electron tunneling modifies only the dispersive character $(\propto \beta)$ of the KdVB equation. Interestingly, in the fine tuning case $\tilde{H} = 2$, the dispersive character of the KdVB equation vanishes, viz., $(\beta = 0)$, and the dynamics of the weakly nonlinear wave is governed by the Burgers equation

$$\frac{\partial \psi}{\partial \tau} + \psi \frac{\partial \psi}{\partial \xi} = \mu \frac{\partial^2 \psi}{\partial \xi^2}, \tag{28}$$

as in the case of an one-dimensional force free ideal and neutral classical fluid.

Moreover, for higher quantum diffraction effect $\tilde{H} > 2$, the derived KdVB equation (27) possesses negative dispersive effect $(\beta < 0)$ as in the case of "oblique" shock waves in a magnetized plasma and also in non-linear transmission lines.

B. Analytical and numerical solutions

The Burgers term in Eq. (27) implies the possibility of the existence of a shock structure. The KdVB equation is not exactly integrable system and hence, exact analytical solutions of the KdVB are not possible. A particular type of solution of the KdVB is possible, which exhibits only the monotonic shock structure. Actually, a dispersive shock wave is generated in a plasma when wave breaking due to the nonlinearity is balanced by the combined action of dispersion and dissipation. In the absence of dissipation balancing the dispersive effect one obtains the generation of solitons described by the KdVB equation. On the other hand, when dissipation dominates, the shock front exhibits a monotonic transition of the plasma density, while the shock transition is of oscillatory nature when the dissipation is weak. To study the nature of the solution[35] of Eq. (27) for $0 \le \tilde{H} < 2$, we transform this equation to the wave frame

$$\zeta = \xi - V\tau = \frac{\sqrt{\epsilon}\,[x - v_{T_i}(U + \epsilon V)t]}{\lambda_{D_i}}$$

with a frame velocity V and then integrate the transformed equation with respect to ζ subject to the boundary conditions ψ, $d\psi/d\zeta$, and $d^2\psi/d\zeta^2 \to 0$ as $|\zeta| \to \infty$. This finally leads to the following equation:

$$\frac{d^2\psi}{d\zeta^2} = \left(\frac{V}{\beta}\right)\psi - \left(\frac{1}{2\beta}\right)\psi^2 + \left(\frac{\mu}{\beta}\right)\frac{d\psi}{d\zeta}. \tag{29}$$

Equation (29) has a well-known mechanical analogy; it describes a damped anharmonic oscillator where ψ plays a role of the generalized coordinate and ζ plays the role of time. In the $(\psi,\ d\psi/d\zeta)$ plane, Eq. (29) has two singular points $(\psi = 0,\ d\psi/d\zeta = 0)$ and $(\psi = 2V,\ d\psi/d\zeta = 0)$. The former corresponds to the equilibrium downstream state and latter corresponds to the upstream state. The singular point (0, 0) is always a saddle point. Actually, if we assume that for $\zeta = \infty(\xi = \infty)$, the particle was located at $\psi = 0$, then at $\zeta = -\infty(\xi = -\infty)$ it appears at the point $\psi = 2V$. Thus, the solution describes a shock like structure. The shock strength is related to the extreme values (upstream and downstream) by

$$\text{Shock strength} = \psi(-\infty) - \psi(+\infty) = 2V.$$

The corresponding Mach number M is

$$M = \frac{\text{nonlinear wave velocity}}{\text{linear wave velocity}} = 1 + \epsilon\left(\frac{V}{U}\right),$$

which is independent of the dispersion.

To find the nature of the shock structure, we investigate the asymptotic behavior of the solution of Eq. (29). For this purpose, we substitute $\psi = 2V + \tilde{\psi}$, where $2V \gg \tilde{\psi}$ into Eq. (29) and then linearize to obtain

$$\frac{d^2\tilde{\psi}}{d\zeta^2} - \left(\frac{\mu}{\beta}\right)\frac{d\tilde{\psi}}{d\zeta} + \left(\frac{V}{\beta}\right)\tilde{\psi} = 0.$$

The solutions of this equation are proportional to $\sim \exp(p\zeta)$,[35] where

$$p = \frac{\mu}{2\beta} \pm \sqrt{\left(\frac{\mu^2}{4\beta^2} - \frac{V}{\beta}\right)}.$$

It follows from this equation that the singular point $(2V,\ 0)$ is a stable focus for $\mu^2 < 4V\beta$ that always corresponds to the oscillatory shock structures (dispersion dominates over dissipation) as shown in Fig. 3. On the other hand, the singular point is a stable node for $\mu^2 > 4V\beta$, which always corresponds to the monotonic shock structure (dissipation dominates over dispersion), as shown in Fig. 4. In terms of the Mach number M (defined above), the conditions for oscillatory and monotonic shock structures can be written as

$$M \gtrless 1 + \frac{\eta^{*2}}{16U\beta}.$$

In the case with $\tilde{H} = 2$, the above equation (27) reduces to the well known Burgers' equation (28), which is exactly integrable and possesses the following monotonic shock like solution

$$\psi = V\left[1 - \tanh\left(\frac{V\zeta}{2\mu}\right)\right], \tag{30}$$

where V and $2\mu/V$ are the amplitude and width of the shock, respectively.

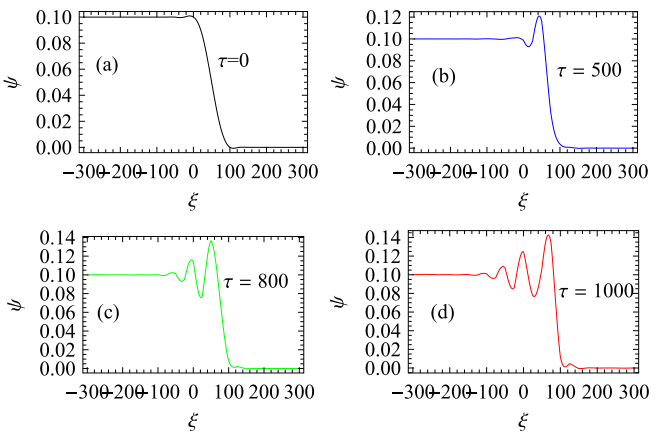

FIG. 3. Evaluation of nonanalytic initial data, a step function, into an oscillatory (dispersive) shock. The upstream value is $A(2V = 0.1)$, giving shock speed $V = 0.05$. The Burgers coefficient $\mu = 0.03$, the dispersion coefficient $\beta = 3$, and the quantum diffraction parameter $\tilde{H} = 0.2$. At $\tau = 1000$, the oscillatory shock is fully developed.

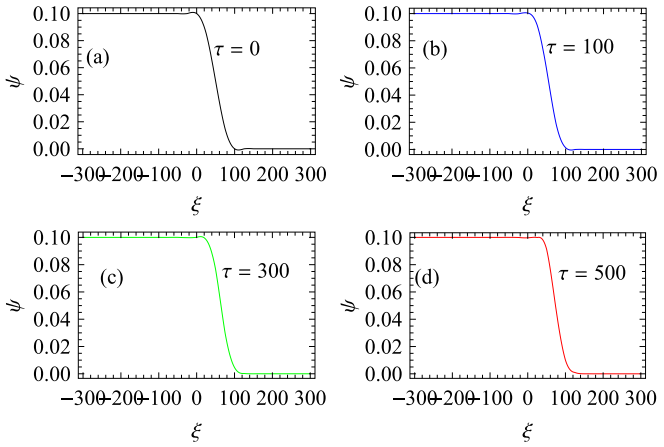

FIG. 4. Evaluation of a monotonic shock for $\tilde{H} = 2$. This implies $\beta = 0$. The other parameters are same as in Fig. 3.

In the case with $\tilde{H} > 2$, we have the KdVB equation (27) with negative dispersion for the weakly nonlinear wave. We can obtain the KdVB equation with positive dispersion by replacing $\psi \to -\psi$ and $\xi \to -\xi$.[36] The sign of the dispersion only determines the direction of the propagation of the wave and therefore the above investigations for $0 \le \tilde{H} < 2$ to study the shock wave in SCQP can be equally applied to a medium with negative dispersion.[35] The difference between the KdVB with positive and negative dispersion is in the direction of propagation only.[35,36]

Therefore, here we solve the KdVB equation (27) numerically for $\beta > 0$. For the time-dependent numerical solution, we use the following initial step-like waveform:

$$\psi(\xi,0) = \begin{cases} A & \text{for } \xi \le 0 \\ \frac{A}{2}(1+\cos k\xi) & \text{for } 0 < \xi < \pi/k \\ 0 & \text{for } \xi \ge \pi/k, \end{cases}$$

where A and k are the initial amplitude and wave number, respectively. The value of k determines the temporal evolution for fixed A. The wave evolves quickly (slowly) for large (small) value of k. Equation (27) is solved within the spatial interval $\xi \in [-L, L]$ with the above initial condition and the boundary conditions: $\psi(-L,\tau) = A$, $\psi(L,\tau) = 0$, and $\psi_\xi(-L,\tau) = 0 = \psi_\xi(L,\tau)$. To obtain adequate results for the computation, we take $L = 300$, $A = 0.1$, and $k = \pi/100$.

In the linear analysis, we have seen that the *hydrodynamic regime* is achieved only in the range $1 < \Gamma_i < 10$. In this range of Γ_i, the Burgers term $\mu \sim 10^{-2}$ and the coefficient of dispersion $\beta \sim 1 - 3$ for $0 \le \tilde{H} < 2$ and $0 < \theta \le 1$. This numerical estimation confirms the existence of an oscillatory shock, as shown in Fig. 3. The comparison between the curves (c) and (d) in Fig. 3 shows that the oscillatory shock is fully developed at $\tau = 1000$. The time-dependent solution for $\tilde{H} = 0$ is shown in Fig. 4. This figure shows the monotonic nature of the shock, which is well agree with the analytical solution (30). Thus, the time-dependent numerical solutions, as shown in Figs. 3 and 4, exhibit the evolution of nonanalytic initial data to the steady-state solutions predicted by the time-independent analysis.

V. DISCUSSIONS AND CONCLUSIONS

In this paper, we have derived a general dispersion relation for the LF-ES in two-component (electron-ion) SCQPs. The effects of ion-ion correlations on weakly nonlinear waves are also discussed. The investigation supports the existence of dispersive (oscillatory) shock wave due to ion-ion correlations in a SCQP. The ion thermal effect, temperature ratio, and quantum diffraction effect due to electron tunneling significantly modify the dispersive character of the wave. Even it changes the character of the shock wave from dispersive to monotonic nature.

All the modes discussed here are longitudinal ($\nabla \times \mathbf{v} = 0$) in nature. However, in strongly coupled two-component plasma there also exists another low-frequency transverse ($\nabla \cdot \mathbf{v} = 0, \nabla \times \mathbf{v} \neq 0$) mode, known as ion transverse (shear) mode[30] in the kinetic regime ($\omega\tau_m \gg 1$). One can easily obtain the shear mode spectrum by taking the curl of the linearized ion equation of motion (1) and $\nabla \times \mathbf{E}$ contribution from Maxwell's equation. In this mode electron transverse susceptibility is irrelevant and as a matter of fact, the quantum diffraction due to electron tunneling has no impact on the ion shear mode spectrum for homogeneous plasmas.

A SCQP is a high-energy-density nonideal plasma. One of the most important characteristic property of such plasma is the collective nature of its behavior.[5] The theory predicts qualitatively new physical effects (plasma phase transitions, metallization, "cold" ionization, etc.)[5] in such SCQPs. The results of the present investigation could be useful for understanding collective oscillations in SCQPs. In particular, let us consider the interior of white dwarfs.[4] The expected plasma compositions are C^{6+} $[O^{8+}]$ ions with the physical parameters $n_{e0} = 2 \times 10^{32}\mathrm{m}^{-3}$ $[6.6 \times 10^{32}\mathrm{m}^{-3}]$ and $T_e = 40T_i = 8.6 \times 10^2\mathrm{eV}$. These values estimate $\Gamma_i \approx 127(Z = 6)$ $[202(Z = 8)]$ implying $\chi_{e(i)} \gg 1(\ll 1)$. The present investigation [Fig. 2(b)] reveals that for these parameters ($\Gamma_i \gg 100$), only the *kinetic modes* exist in such plasmas and ionic structure formation takes place with the degenerate electron background, which has been observed in the interior of white dwarf.[10]

The experimental observations on SCQPs are rare in the literature. Thus, the present theoretical investigation might have some bearing to observe the linear as well as nonlinear ES modes that can participate in the scattering processes involving intense laser beams in the forthcoming high-energy density compressed plasma experiments dealing with inertial confinement fusion schemes.

[1]F. Haas, *Quantum Plasma Physics: An Hydrodynamic Approach* (Springer, New York, 2011).
[2]P. K. Shukla and B. Eliasson, Rev. Mod. Phys. **83**, 885 (2011).
[3]D. Lai, Rev. Mod. Phys. **73**, 629 (2001).
[4]S. L. Shapiro and S. A. Teukolsky, *Black Holes, White Dwarfs, and Neutron Stars: The Physics of Compact Objects* (Wiley, New York, 1983).
[5]V. E. Fortov, Phys. Usp. **52**, 615 (2009).
[6]M. Marklund and P. K. Shukla, Rev. Mod. Phys. **78**, 591 (2006).
[7]M. Marklund and G. Brodin, Phys. Rev. Lett. **98**, 025001 (2007).
[8]G. Brodin, M. Marklund, and G. Manfredi, Phys. Rev. Lett. **100**, 175001 (2008); P. K. Shukla, Nat. Phys. **5**, 92 (2009).
[9]F. Hass, G. Manfredi, and M. Fiex, Phys. Rev. E **62**, 2763 (2000).
[10]L. Segretain, Astron. Astrophys. **310**, 485 (1996).
[11]P. K. Shukla and B. Eliasson, Phys. Usp. **53**, 51 (2010); S. V. Vladimirov and Yu. O. Tsyhetskiy, *ibid.* **54**, 1243 (2011).
[12]T. C. Killian, S. Kulin, S. D. Orezee, and S. I. Rojston, Phys. Rev. Lett. **83**, 4776 (1999); T. C. Killian, M. Lin, S. Kulin, S. Bergson, and S. I. Rojston, *ibid.* **86**, 3759 (2001).
[13]B. DeMarco and D. S. Jin, Science **285**, 1703 (2000).
[14]M. S. Murillo, Phys. Rev. Lett. **87**, 115003 (2001).
[15]F. Hass, L. G. Garcia, J. Goedert, and G. Manfredi, Phys. Plasmas **10**, 3858 (2003).
[16]N. Chakrabarti, M. S. Janaki, M. Dutta, and M. Khan, Phys. Rev. E **83**, 016404 (2011).
[17]C. L. Gardner and C. Ringhofer, Phys. Rev. E **53**, 157 (1996).
[18]G. Manfredi and F. Hass, Phys. Rev. B **64**, 075316 (2001).
[19]G. Manfredi, Fields Inst. Commun. **46**, 263 (2005); P. K. Shukla and B. E. Eliasson, Phys. Rev. Lett. **96**, 245001 (2006); *ibid.* **99**, 096401 (2007); D. Dastgeer and P. K. Shukla, *ibid.* **99**, 125002 (2007).
[20]M. Rosenberg and G. Kalman, Phys. Rev. E **56**, 7166 (1997).
[21]P. K. Kaw and A. Sen, Phys. Plasmas **10**, 3552 (1998).
[22]H. Ohta and S. Hamaguchi, Phys. Rev. Lett. **84**, 6026 (2000).
[23]M. S. Murillo, Phys. Rev. Lett. **85**, 2514 (2000).
[24]Z. Donkó, G. J. Kalman, and P. Hartmann, J. Phys.: Condens. Matter **20**, 413101 (2008).
[25]M. S. Janaki and N. Chakrabarti, Phys. Plasmas **17**, 053704 (2010).
[26]P. Vieillefosse and J. P. Hansen, Phys. Rev. A **12**, 1106 (1975).
[27]W. L. Slattery, G. D. Doolen, and H. E. DeWitt, Phys. Rev. A **21**, 2097 (1980); **26**, 2255 (1982).
[28]S. Ichimaru, *Statistical Plasma Physics, Condensed Plasmas* Vol. II (Addison Wesley, New York, 1994).
[29]K. I. Golden, Phys. Rev. A **35**, 5278 (1987).
[30]M. A. Berkovsky, Phys. Lett. A **166**, 365 (1992); J. Plasma Phys. **50**, 359 (1993).
[31]Y. I. Frenkel, *Kinetic Theory of Liquids* (Clarendon, Oxford, 1946).
[32]V. M. Atrazhev and I. T. Iakubov, Phys. Plasmas **2**, 2624 (1995).
[33]L. D. Landau and E. M. Lifshitz, *Statistical Physics, Part I* (Butterworth-Heinemann, Oxford, 1980).
[34]D. Bohm and T. Staver, Phys. Rev. **84**, 836 (1951).
[35]V. I. Karpman, *Nonlinear Waves in Dispersive Media* (Pergamon, London, 1975).
[36]A. Jeffery and T. Kakutani, SIAM Rev. **14**, 582 (1972).